Received: 26 November 2019 | Revised: 8 May 2020 | Accepted: 11 May 2020 | Published on: 8 June 2020

DOI: 10.1002/joc.6668

RESEARCH ARTICLE

International Journal of Climatology RMetS

Best practices for estimating near-surface air temperature lapse rates

A. C. Lute[1] | **John T. Abatzoglou**[2,3]

[1]Water Resources Program, University of Idaho, Moscow, Idaho

[2]Management of Complex Systems Department, University of California, Merced, Merced, California

[3]Department of Geography, University of Idaho, Moscow, Idaho

Correspondence
A. C. Lute, Water Resources Program, University of Idaho, 875 Perimeter Dr., Moscow, ID 83844.
Email: alute@uidaho.edu

Funding information
National Science Foundation, Grant/Award Number: 1249400

Abstract

The near-surface air temperature lapse rate is the predominant source of spatial temperature variability in mountains and controls snowfall and snowmelt regimes, glacier mass balance, and species distributions. Lapse rates are often estimated from observational data, however there is little guidance on best practices for estimating lapse rates. We use observational and synthetic datasets to evaluate the error and uncertainty in lapse rate estimates stemming from sample size, dataset noise, covariate collinearity, domain selection, and estimation methods. We find that lapse rates estimated from small sample sizes (<5) or datasets with high noise or collinearity can have errors of several °C km^{-1}. Uncertainty in lapse rates due to non-elevation related large-scale temperature variability was reduced by correcting for spatial temperature gradients and restricting domains based on spatial clusters of stations. We generally found simple linear regression to be more robust than multiple linear regression for lapse rate estimation. Finally, lapse rates had lower error and uncertainty when estimated from a sample of topoclimatically self-similar stations. Motivated by these results, we outline a set of best practices for lapse rate estimation that include using quality controlled temperature observations from as many locations as possible within the study domain, accounting for and minimizing non-elevational sources of climatic gradients, and calculating lapse rates using simple linear regression across topoclimatically self-similar samples of stations which are roughly 80% of the station population size.

KEYWORDS

climate, elevation-dependent warming, error, lapse rate, linear regression, temperature, uncertainty

INTRODUCTION

Accurate estimates of air temperature are essential for understanding and modelling environmental processes in mountain regions. The predominant source of mesoscale to microscale spatial temperature variability in mountains is associated with elevation through the near-surface air temperature lapse rate. In contrast to the free-air lapse rate that represents temperature changes along a vertical profile through the boundary layer and into the free atmosphere, the near-surface air temperature lapse rate (hereafter, lapse rate) represents temperature variability within the surface layer (McCutchan, 1983). The lapse rate is therefore a key parameter for resolving local conditions in many environmental models that consider topoclimate variability in montane regions. However, guidance on estimating lapse rates is lacking, despite the fact that hydrological and ecological modelling efforts can be highly sensitive to the choice of lapse rate

parameter used to infer fine-scale spatial temperature fields (Sekercioglu *et al*., 2008; Gardner and Sharp, 2009; Immerzeel *et al*., 2014). For example, Minder *et al*. (2010) showed that the application of contrasting lapse rates (−4 and −6.5°C km^{-1}) to a snow model resulted in a 1-month difference in snowmelt commencement in the Washington Cascades, United States. Accurate lapse rate estimates are also needed to detect and project future elevation dependent warming (Pepin *et al*., 2015).

In practice, the lapse rate is often assumed to equal the mean environmental lapse rate (MELR) of −6.5°C km^{-1}. Yet, observations show large variability of lapse rates geographically, seasonally, diurnally, and with elevation (Rolland, 2003; Lundquist and Cayan, 2007; Shen *et al*., 2016; Navarro-Serrano *et al*., 2018). The latter results in nonlinear lapse rates, although this is rarely acknowledged in modelling contexts. Mechanistic explanations for lapse rate variability include radiative processes, thermodynamics, and atmospheric dynamics (Harding, 1979; Blandford *et al*., 2008; Kattel *et al*., 2013; Navarro-Serrano *et al*., 2018).

Despite basic understanding of these processes, it remains difficult to constrain lapse rate estimates with observational data. Figure 1 illustrates this challenge showing summer temperatures across a longitudinal transect of the Oregon Cascades, United States. Station observations are a sample of the spatial temperature field. The default assumption that the full population of station observations is optimal for estimating the lapse rate has not been evaluated. Lapse rate estimates can be confounded by varied topoclimatic controls across a region of interest, which may help explain the diversity of lapse

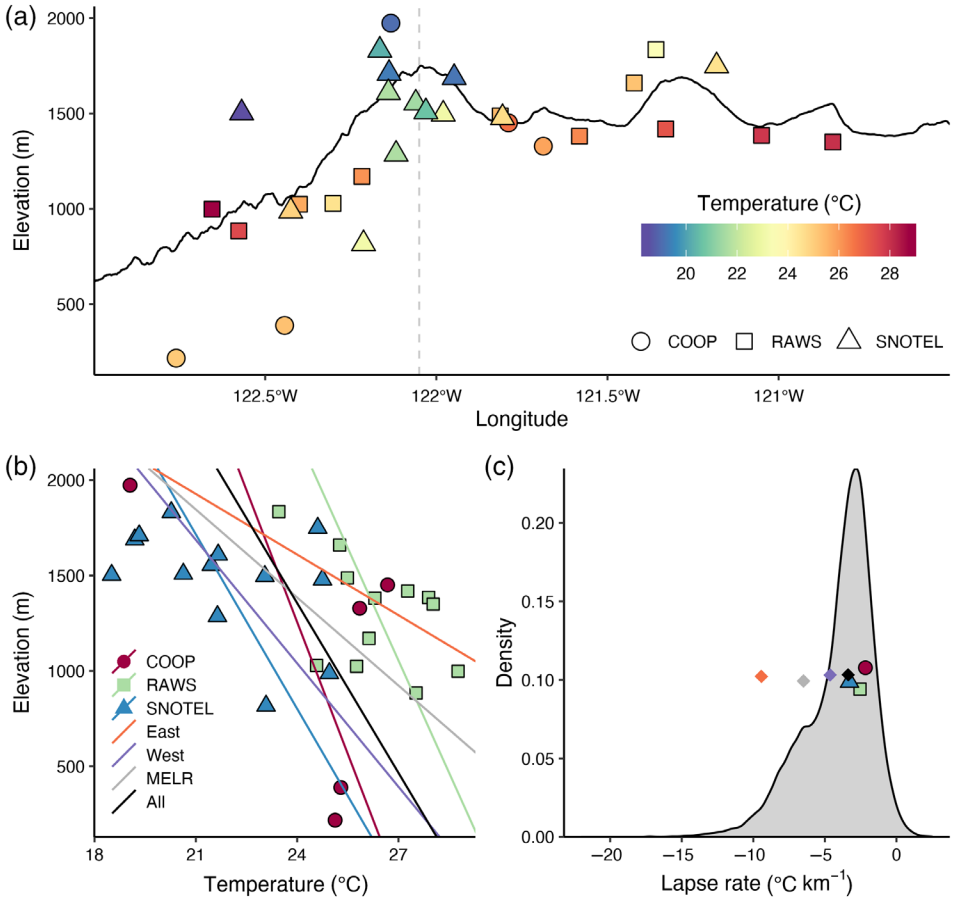

FIGURE 1 (a) Black line shows mean elevation across longitude over the study domain of the Oregon Cascades, United States (42.8–44°N, 120.5–123°W). Coloured points show mean summer maximum temperature from 30 weather stations with symbols indicating the originating network. Vertical grey dashed line marks the maximum elevation of the transect and divides the stations into west and east groups. (b) Examples of lapse rates calculated from these stations, including using only sites from the US Cooperative Observer Program (COOP), the US Interagency Remote Automatic Weather Stations (RAWS) network, the US Natural Resources Conservation Service Snowpack Telemetry (SNOTEL) network, only sites east or west of the divide, the mean environmental lapse rate (MELR, −6.5 °C km^{-1}), or all stations (n = 30). (c) Distribution of lapse rates estimated from 15,000 samples of 10 stations from the full population shown in (a). Colours and symbols in (c) indicate lapse rates shown in (b). Vertical jitter has been added to points in (c)

rates estimated using varied sample configurations (e.g., Figure 1b,c). Hence, while it is conceptually easy to calculate a lapse rate, the statistical approach and station characteristics merit more careful consideration than typically given.

Lapse rates are typically estimated via either simple linear regression (SLR) of temperature on elevation or multiple linear regression (MLR) of temperature on elevation and other covariates using a local population of observations (e.g., Pepin *et al*., 1999; Rolland, 2003; Kattel *et al*., 2013); it remains unclear whether SLR or MLR is more appropriate. Additionally, these approaches may be confounded by factors exogenous to elevation but collinear with elevation, including topographic position, land cover, soil moisture, and snow cover (Rolland, 2003; Dobrowski *et al*., 2009; Kattel *et al*., 2013; Navarro-Serrano *et al*., 2018). Collinearity is common among empirical approaches designed to isolate a single phenomenon and contributes to biased and unstable parameter estimates in SLR and MLR (e.g., Graham, 2003; Dormann *et al*., 2013). Another key consideration in calculating lapse rates is sample size. Studies have used as few as two up to tens of stations (Kirchner *et al*., 2013; Li *et al*., 2013). A further question is which stations should be used. Recognizing the role of topoclimatic factors in both determining and, in the context of collinearity, confounding lapse rates it may be appropriate to estimate lapse rates from stations with similar topoclimatic characteristics.

Given the importance of accurate lapse rates to environmental understanding and modelling, efforts to improve lapse rate estimation methods offer cascading benefits. This study quantifies the uncertainty and error in lapse rate estimates stemming from dataset characteristics and methodological choices by complementing observational data with synthetic data. In addition to standard SLR and MLR methods for lapse rate estimation we introduce a novel method that identifies samples of stations that are topoclimatically self-similar. Finally, we provide recommendations on best practices for lapse rate estimation that are applicable in any geographic or temporal context.

1 | DATA

A collection of stations traversing the Cascade Mountains of Oregon, United States (42.8–44°N, 120.5–123°W) was selected to exemplify complex terrain and land surfaces typical of mountain regions (Figure 2). The western, maritime portion of the domain is largely mesic and forested whereas the eastern portion in the rain shadow of the Cascade Mountains is largely semi-arid with mixed forest and shrubland. Observational data were complemented by a suite of synthetic datasets with prescribed lapse rates. The following sections provide details of the synthetic, observational, and covariate datasets.

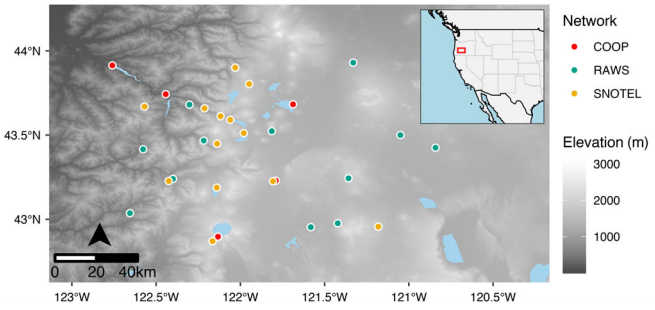

FIGURE 2 Oregon Cascades study area. Red box in inset map shows location of Oregon Cascades study area in Western North America. The 30 meteorological stations used in this study are indicated by markers according to the observation network. Light blue polygons are waterbodies

1.1 | Synthetic datasets

The true lapse rate in a given observational setting is rarely known, impeding efforts to formally evaluate empirical lapse rate approaches. As an alternative, we developed synthetic temperature datasets with a prescribed lapse rate and fully quantified covariates. Nine synthetic datasets were developed that considered different levels of dataset noise and topoclimatic collinearity with elevation. Synthetic datasets had the same number of 'stations' ($n = 20$) at the same elevations with a prescribed lapse rate of -6.5°C km^{-1}. Dataset noise (e.g., sensor error, data transcription errors, temperature variations not explained by other covariates) was quantified as the standard deviation of the random error term and was prescribed at three levels: 0.1, 1, and 2°C. Dataset collinearity was quantified as the correlation (r) between elevation and a prescribed covariate, solar radiation, at three levels: 0.00, 0.30, and 0.60.

Station temperatures were calculated as the sum of the temperature effects of three conceptual covariates and the random error term:

$$T_{s,ds} = T_{elev_{s,ds}} + T_{srad_{s,ds}} + T_{coast_{s,ds}} + T_{\varepsilon s,ds} \quad (1)$$

where T is the temperature at station s in dataset ds, and T_{elev}, T_{srad}, T_{coast}, and T_{ε} are the temperature effects of elevation, solar radiation, distance from coast, and random error, respectively. Further details can be found in Supplementary information S1.

1.2 | Observational datasets

Daily minimum (Tmin) and maximum temperature (Tmax) during September 1, 2005–August 31, 2015 for stations in Oregon were acquired from the Global Historical Climatology Network – Daily dataset (GHCND v3; Menne *et al*., 2012). We discarded values that were flagged for quality control. The remaining data were subject to completeness requirements such that stations were included if all years reported ≥85% of daily values (Daly *et al*., 2008). Seasonal (DJF, MAM, JJA, SON) average temperatures were computed for seasons with ≥85% of daily values reported, years with seasonal values reporting <85% of daily values were set to missing, and annual and seasonal averages at each station were computed from at least 7 (out of a possible 10) data points. This resulted in 30 stations with Tmax and Tmin records covering the Oregon Cascades region of interest and spanning elevations from 217 to 1974 m (Figures 1 and 2). The dataset includes stations from the U.S. Cooperative Observer Program (COOP) network ($n = 5$), the U.S. Natural Resources Conservation Service Snowpack Telemetry (SNOTEL) network ($n = 13$), and the U.S. Interagency Remote Automatic Weather Station (RAWS) network ($n = 12$).

We selected covariates representative of known sources of non-elevational temperature variability in mountains (Table 1). Details of covariate data sources and calculations are provided in Supplementary information S1. Covariates were estimated for each station, and in the case of time varying metrics, for seasonal and annual averages.

TABLE 1 Covariates used to account for non-elevational effects on temperature

Covariate	Relevant process	Data source
Solar radiation	Surface energy budget	WRF
Topographic convergence index (TCI)	Cold air pooling, coupling to free atmosphere	SRTM
Cloud cover	Shading during daytime, enhanced longwave radiation	MODIS
Orographic upslope wind index (windex)	Cloud cover, latent heating due to upslope condensation	ERA-Interim Reanalysis, SRTM
Distance from coast	Moisture availability, cloud cover, Bowen ratio	
Waterbody index	Surface energy budget	NHDPlus V2
Free-air temperature	Broad scale atmospheric conditions	ERA-Interim Reanalysis
Free-air lapse rate	Atmospheric stability	ERA-Interim Reanalysis

2 | METHODS

2.1 | Regression approaches

We employ two common approaches to estimate temperature lapse rates: simple linear regression (SLR) and multiple linear regression (MLR). In SLR, temperature is regressed on elevation, such that

$$T = \beta_0 + \beta_1 \times elev + \varepsilon \quad (2)$$

where T is the temperature at a given place and time, β_0 is the temperature at reference sea level, β_1 is the lapse rate, *elev* is the elevation, and ε is the error. This approach assumes that temperature varies only as a function of elevation, disregarding additional topoclimatic factors known to affect temperature. Non-elevational factors that influence temperature but are not correlated with elevation will be subsumed within the error term. However, if these other factors are correlated with elevation, then SLR will alias these factors, making the lapse rate a derivative of temperature with respect to elevation, instead of a partial derivative.

In MLR, temperature is regressed on elevation and other variables, such that

$$T = \beta_0 + \beta_1 \times elev + \beta_2 \times X_2 + \ldots + \beta_n \times X_n + \varepsilon \quad (3)$$

where the additional $n - 1$ terms β_2 through β_n are coefficients for the additional $n - 1$ predictor variables X_2 through X_n. The present study uses covariates of elevation, solar radiation, and distance from coast, which explain a large portion of temperature variability across the domain (Figure S1). The number of covariates was limited to three and MLR lapse rates were not calculated for samples of <4 stations for this example in order to avoid overfitting. A potential hazard in the MLR approach is the assumption of noncollinearity of covariates; collinearity between elevation and other predictor variables can produce large uncertainties in estimated lapse rates (Dormann *et al*., 2013).

We further evaluated the effect of sample size on the robustness of lapse rates by running calculations for every combination of stations from two to the population

size. Due to computational limitations, we restricted the number of station combinations (i.e., samples) for a given sample size to 15,000.

2.2 | Domain selection

Spatial variability of lapse rates has been documented for many regions (Wolfe, 1992; Rolland, 2003; Li *et al*., 2013), motivating a domain selection process for grouping stations based on climatic and physiographic factors. We used an empirical clustering approach based on known regional climate gradients and previous work documenting windward-leeward contrasts in lapse rates (Minder *et al*., 2010). Regionalizing climate stations is commonly done to isolate stations in terms of certain climate phenomenon (Abatzoglou *et al*., 2009). Clustering was based on covariates that capture large scale climatic and moisture gradients: the upslope flow index (hereafter, windex) and the free-air lapse rate. The windex provides an indication of linear orographic flow (product of the lower tropospheric flow and local terrain gradient, see Supplementary information S1) and the free-air lapse rate provides an indication of broad scale atmospheric stability calculated directly from pressure level reanalysis or radiosonde data (Minder *et al*., 2010). Clusters based on seasonal values of the 40 km windex and free-air lapse rates were assessed using a k-means approach with $k = 2$ and 10 random starting clusters. Lapse rates estimated from the resulting clusters were compared with one another and with lapse rates estimated from the full population.

2.3 | Accounting for regional climate

Ideally lapse rates are estimated over small domains with little contrast in regional climate, however the paucity of observational stations in mountains often necessitates the use of larger domains (>100 km). Large domains may have significant spatial climatic gradients not directly tied to elevation (e.g., solar radiation, circulation patterns, continentality), making it difficult to isolate elevation-temperature relationships. In these contexts, it is useful to consider near-surface temperatures as a function of regional climate and topoclimatic siting (Lundquist *et al*., 2008; Dobrowski *et al*., 2009; Sadoti *et al*., 2018). This framing contrasts with traditional SLR and MLR methods which do not recognize the effect of regional climate on near-surface temperature.

We use free-air temperatures collocated with stations and at a fixed elevation (2,500 m was used in this analysis, the approximate height of the Cascade crest) derived from ERA-Interim (Supplementary information S1) as a proxy for spatially varying temperatures that do not entrain elevational controls. Spatially corrected station temperatures (T_{sc}) are calculated as the difference between station temperatures and free-air temperatures. While previous studies have used free-air temperatures to account for temporal temperature variability (e.g., Dobrowski *et al*., 2009), here we use free-air temperatures to account for spatial temperature variability. We evaluate lapse rates estimated from SLR in which T_{sc} is substituted for station temperature as the dependent variable.

2.4 | Identifying influential stations

Data points with high leverage and an anomalous predictor-response value combination can strongly influence linear regression coefficients (Altman and Krzywinski, 2016). In the context of lapse rates, the highest and lowest elevation stations can exert outsized influence on the lapse rate estimate if their temperatures are poorly predicted by a model based on the other stations. We quantify the influence of each station using Cook's Distance (Cook, 1977). Stations with Cook's Distances exceeding four divided by the population size in all seasons are considered influential and are considered for exclusion from lapse rate calculations (Altman and Krzywinski, 2016). For brevity, we only evaluate station influence for a subset of the Oregon Cascades stations.

2.5 | Topoclimatic dissimilarity approach (TDA)

To improve lapse rate estimates in the context of collinear covariates, one can minimize the temperature variance explained by non-elevational factors. One way to accomplish this is to a priori develop lapse rates based on stations that occupy similar topoclimatic siting for covariates except elevation. For example, solar radiation will be a less important predictor of inter-station variability in Tmax for a sample where all sites have similar radiational loading than in a sample with large differences in solar radiation. These arguments form the basis for a new lapse rate estimation method, termed the Topoclimatic Dissimilarity Approach (TDA). The TDA is conceptually similar to the Parameter-elevation Relationships on Independent Slopes Model (PRISM; Daly *et al*., 2002), in that stations are selected or weighted based on topoclimatic characteristics, however the specific methods and goals differ.

The TDA is a sample selection algorithm which preferentially minimizes the range of values of non-elevational

factors according to the amount of temperature variability the factor explains. The correlations (r_v) between each covariate (v) and temperature across the full population of stations are used to weight each covariate. Weightings are applied as the square root of the absolute values of r_v. Using the full population, each covariate is then converted to standardized anomalies so that covariates can be compared. We calculate the range of standardized anomalies (R_v) for each covariate across each sample. Elevation ranges are subtracted from the maximum elevation range of all the samples to allow the algorithm to maximize the range of elevation while minimizing the ranges of all other covariates. A topoclimatic dissimilarity metric (TD) is then computed as the weighted maximum distance for each sample:

$$TD = \sum_{v=1}^{p} \sqrt{|r_v|} \times R_v \quad (4)$$

where p is the number of covariates evaluated. TD quantifies the topoclimatic dissimilarity of each sample, with lower values representing more topoclimatically self-similar samples. In subsequent analyses, TDA results are presented grouped in deciles of TD to elucidate the potential value of self-similar samples. Covariates included in the TDA algorithm as used in this study are elevation, TCI, cloud cover, windex, distance from coast, and the waterbody index for the observational data and elevation, solar radiation, and distance from coast for the synthetic datasets. This algorithm is available as an R script at https://github.com/abbylute/lapse_rate_TDA.

In addition to comparing lapse rates from TDA to lapse rates from randomly sampled stations, we evaluated potential advantages of using TDA compared to using SLR with an entire population to determine whether the benefits of TDA outweighed the benefits of a larger sample. For each synthetic dataset, we drew all possible subpopulations of each size (N_{sub}) from 4 to 19. For N_{sub} with >100 subpopulations, we randomly selected 100 from the list of all possible subpopulations. From each subpopulation, we similarly drew up to 100 random samples of each size from 2 to $N_{sub} - 1$. We applied the TDA to each of these subpopulation-sample size combinations. Finally, we compared the error of the median lapse rates from the samples with TD in the lowest decile to the lapse rate error from SLR applied to the subpopulations.

2.6 | Assessment metrics

Lapse rate error was quantified as the difference between the specified lapse rate (-6.5°C km^{-1} for the synthetic datasets) and the estimated lapse rate. We use mean absolute error (MAE) to quantify the average lapse rate error and mean error to quantify lapse rate bias. Error was not quantified for the observational dataset because the true lapse rate is unknown.

Lapse rate uncertainty for both the observational and synthetic datasets was quantified as the interquartile range (IQR) of the lapse rate estimates. Differences in uncertainty are used to assess improvements in observational lapse rate accuracy.

Initial results for both datasets are presented for a sample size of 5 since this is representative of sample sizes used in the literature (e.g., Blandford *et al*., 2008; Gardner *et al*., 2009; Kirchner *et al*., 2013; Li *et al*., 2013). Later results are presented for multiple sample sizes or for sample sizes determined to be more appropriate based on intermediate results.

3 | RESULTS AND DISCUSSION

3.1 | Synthetic datasets

3.1.1 | Lapse rate sensitivity to collinearity, dataset noise, sample size, and method

Lapse rate uncertainty and error were typically greater for datasets with high dataset noise, high collinearity, small sample sizes, or when MLR was used (Figures 3 and 4). For samples of 5 stations, we found that increased dataset noise increased the uncertainty and MAE of SLR and MLR lapse rate estimates (Figure 3). Secondly, increased collinearity increased the bias of SLR lapse rate estimates (Figure 3a). The bias was positive in this case due to the way the collinearity was prescribed in the synthetic datasets (i.e., a positive correlation between elevation and solar radiation aliases the lapse rate to other processes). Thirdly, the response of MLR estimates to collinearity was less consistent than for SLR, likely due to interactions with noise which affected the collinearity structure; dataset noise can be aliased by other covariates and contribute to additional collinearity and therefore additional error. Except for cases with low noise (0.1°C), SLR generally outperformed MLR.

We next compared the sensitivity of lapse rate MAE to sample size across the matrix of estimation method, collinearity, and dataset noise. MAE increased with increased collinearity, increased dataset noise, or decreased sample size in almost every case (Figure 4). Firstly, MAE increased exponentially with decreasing sample size and was typically <1°C km^{-1} for sample sizes of at least 5 stations. Small samples were more likely to span a small elevation range (<500 m) than larger

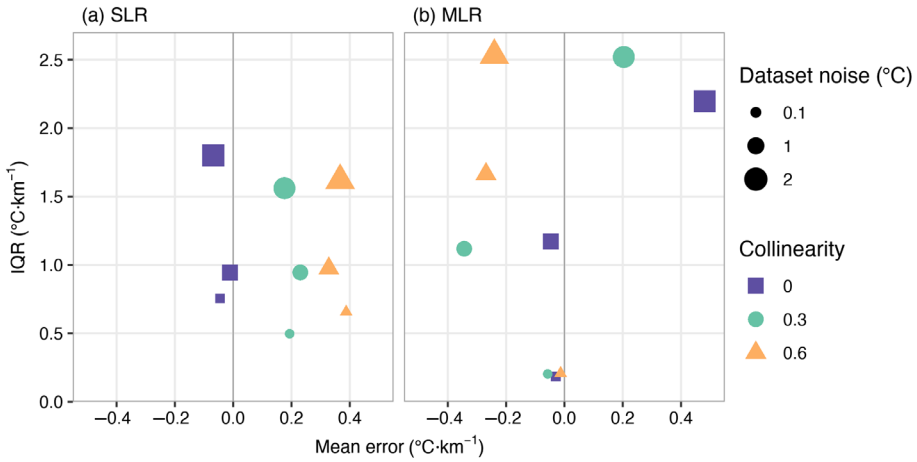

FIGURE 3 Lapse rate mean error (*x*-axis) and interquartile range (*y*-axis) estimated via (a) SLR and (b) MLR for datasets with varying levels of dataset noise (size) and collinearity (colour, shape). Lapse rates are estimated from samples of five stations drawn from each synthetic dataset

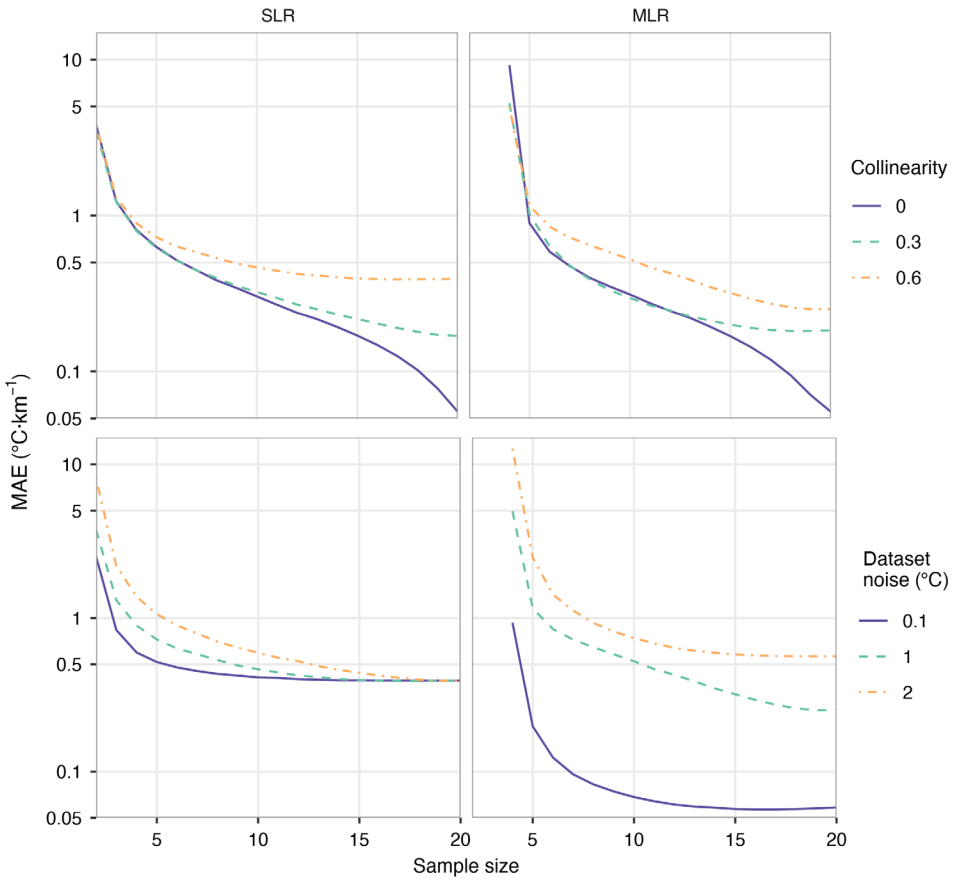

FIGURE 4 MAE of lapse rates (log scale on *y*-axis) estimated from synthetic datasets using SLR (left column) and MLR (right column). MAE is calculated across all possible samples of the sample size indicated on the *x*-axis. In the upper plots each line represents a synthetic dataset with a different collinearity level and with dataset noise of 1°C, in the lower plots each line represents a dataset with a different level of dataset noise and with collinearity of 0.6

samples, which amplified the effect of non-elevational factors on the lapse rate (not shown) and increased uncertainty. Secondly, SLR lapse rate estimates had lower error than MLR estimates for small sample sizes (5 or less), greater collinearity, and greater dataset noise. Small samples can have greater collinearity (both from latent covariates and aliased from dataset noise) than the population as a whole, resulting in larger MAE, particularly for MLR. MLR slightly outperformed SLR for cases with low to moderate dataset noise and collinearity and sample sizes >5. These results mirror conclusions of other statistical efforts that consider the interacting effects of noise, collinearity, sample size, and regression method on the bias and uncertainty of regression coefficients in other disciplines (Mason and Perreault Jr., 1991).

3.1.2 | Application of topoclimatic dissimilarity approach to synthetic datasets

Compared to all samples, the most self-similar samples generally had lower lapse rate MAE and uncertainty

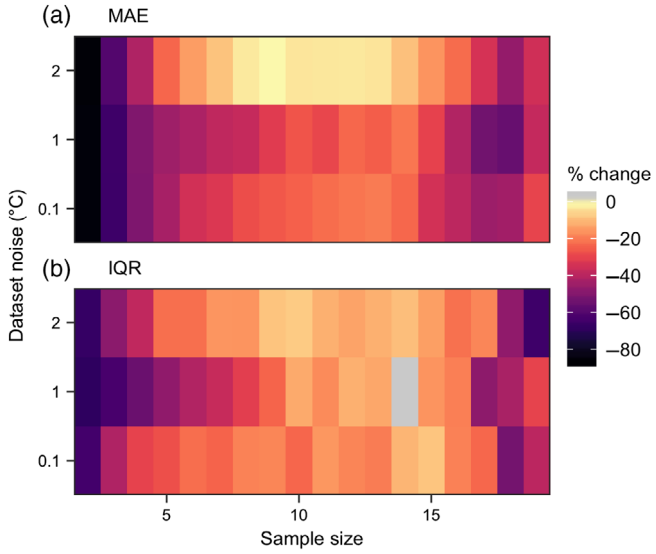

FIGURE 5 Percent change in (a) MAE and (b) IQR between the most similar decile of samples selected using TDA and all samples. Results are shown for lapse rates estimated via SLR from samples of varying sample size (*x*-axis) drawn from datasets with collinearity of 0.3 and varying dataset noise (*y*-axis). Negative values indicate that the most similar decile had lower MAE or IQR than the average sample. Positive values (grey) indicate increased MAE or IQR

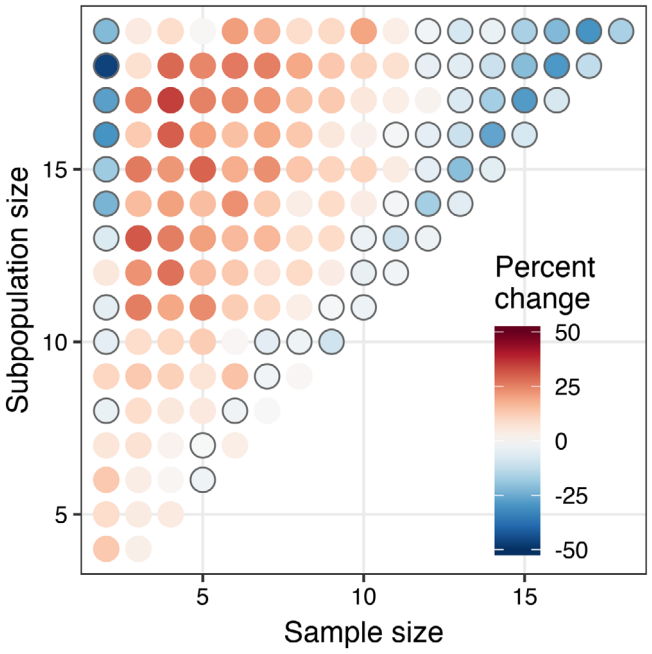

FIGURE 6 Percent difference in MAE between lapse rates of varying sample size (*x*-axis) selected by the TDA (i.e., the median lapse rate from the most similar decile of samples) and lapse rates calculated from the full subpopulations using SLR (subpopulation size shown on *y*-axis). Blue, outlined points indicate reduced MAE. Data is from the synthetic dataset with noise of 1°C and collinearity of 0.6

(Figure 5). The TDA was effective at reducing error and uncertainty for small samples, since small samples from a finite population provide more diversity to choose from than larger samples which have many stations in common and offer limited flexibility. The TDA also reduced error and uncertainty for large samples, which had low error initially (Figure 4), suggesting that omission of just one to a few outlier stations can greatly reduce lapse rate error. Low uncertainty does not necessarily equate to better lapse rates with lower error; it is possible to have low lapse rate uncertainty but large lapse rate error. However, across the synthetic datasets lower IQR typically corresponded to lower MAE (e.g., Figure 5), suggesting that this definition of uncertainty may be a proxy for error in the observational datasets.

The median lapse rate from the most similar decile of samples, evaluated for all sample sizes, dataset noise, and collinearity levels, had absolute error < 0.5°C in 84% of cases, compared to 67% of cases for all possible samples. The median lapse rate from the most similar decile provides a good best guess at the actual lapse rate and the minimum and maximum lapse rates from the most similar decile may be useful as a measure of lapse rate uncertainty.

Median lapse rates from the most similar decile of samples had lower MAE than lapse rates estimated from subpopulation-based SLR in some cases (Figure 6), with MAE being an average of 12% lower (-0.04°C km^{-1}) for subpopulation size >5 and sample size ≥80% of the subpopulation size. Given the larger uncertainty of the observational data (3.5°C km^{-1} on average for the SLR results shown in Figure 7) compared to the synthetic data (1°C km^{-1} for sample size of 5 for datasets with 1°C noise), we expect larger absolute error reduction for the TDA applied to the observational data. In many cases, lapse rates estimated from the TDA using a sample size of 2 had lower error than the full subpopulation, illustrating that it is possible to calculate an accurate lapse rate from only two stations. However, error reduction was more consistent for samples sizes that were roughly ≥80% of the subpopulation size. For the middle range of sample sizes, the TDA was not beneficial; middle range sample sizes had neither the flexibility of small samples to choose the best stations nor the robustness of the larger samples. Finally, for subpopulation sizes roughly ≤5, the TDA was not consistently beneficial. In these cases, the median of lapse rates estimated from all possible station combinations of size 2 to the subpopulation size − 1 typically was as accurate or more accurate than the full subpopulation lapse rate (not shown).

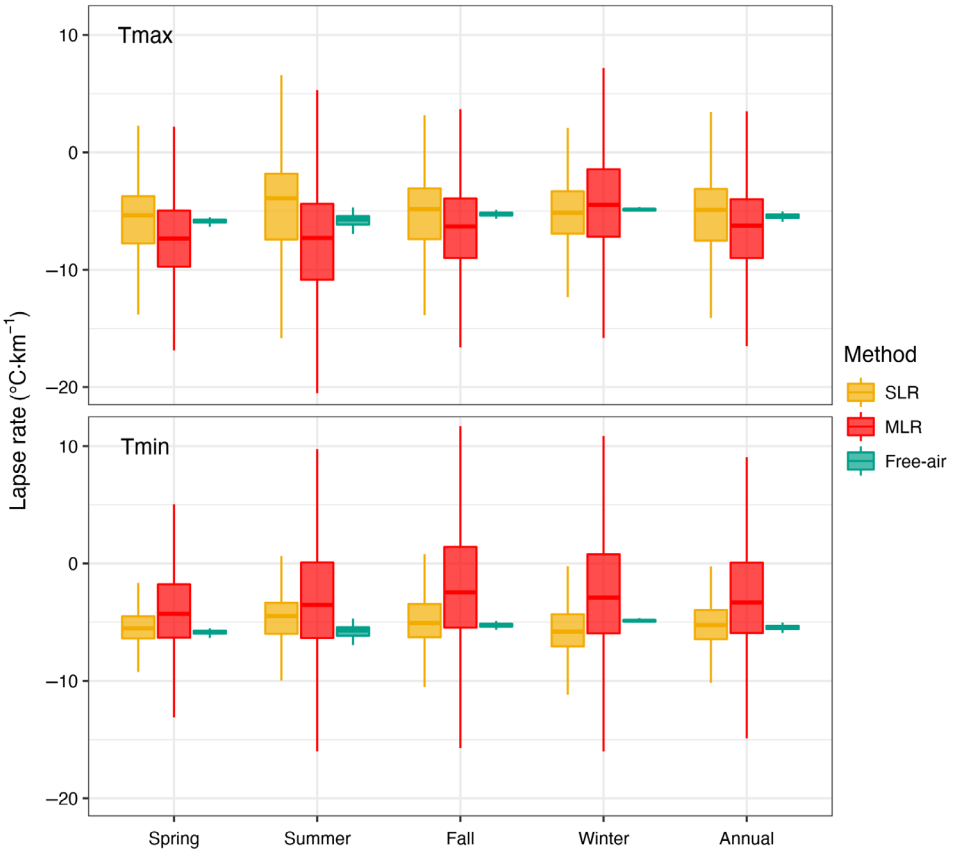

FIGURE 7 Lapse rates calculated from samples of five stations from the 30 stations in the Oregon Cascades dataset for Tmax (top) and Tmin (bottom). Yellow boxes indicate lapse rates calculated via SLR. Red boxes correspond to lapse rates calculated via MLR using elevation, solar radiation, and distance from coast as predictors. Green boxes indicate free-air lapse rates calculated from ERA-Interim reanalysis collocated with stations (see Supplementary information S1 for details) and are the same for Tmax and Tmin

3.2 | Oregon Cascades station dataset

3.2.1 | Lapse rate estimation method and sample size

Seasonal lapse rates estimated via MLR from samples of 5 stations from the Oregon Cascades had uncertainty >5°C km^{-1} (Figure 7). Tmax lapse rates estimated via SLR were generally weaker than those estimated via MLR, while the opposite was found for Tmin. The uncertainty of SLR estimates was generally smaller than for MLR, which is expected since SLR regression coefficient variance is a function of sample size and noise, whereas MLR coefficient variance is additionally a function of collinearity (Mason and Perreault Jr., 1991; Montgomery *et al.*, 2012). Uncertainty increased dramatically for samples smaller than 10 stations (not shown). Combined with the results for the synthetic datasets, these results confirm the hypothesis of Rolland (2003) that small sample sizes can be a source of error in lapse rate estimates.

Free-air lapse rates showed limited seasonality and typically fell between the SLR and MLR estimates for Tmax but were steeper than most SLR and MLR estimates for Tmin. The steeper free-air lapse rates relative to near-surface Tmin lapse rates is likely related to night-time atmospheric decoupling and cold air drainage (Lundquist *et al.*, 2008; Daly *et al.*, 2010).

3.2.2 | Collinearity

One might expect that the predictor variables in the MLR (elevation, solar radiation, and distance from coast) would capture the key processes controlling spatial variability in temperature and provide more refined lapse rate estimates than SLR. However, MLR increased lapse rate uncertainty due to collinearity between elevation and additional predictor variables (e.g., the correlation between elevation and distance from coast was 0.57; Figure S1). Recognizing this collinearity and the large uncertainty in MLR lapse rates (Figure 7), we focus on SLR lapse rates for the remainder of the paper. For brevity, we only present results for Tmax to illustrate our methods.

3.2.3 | Accounting for spatial variability of lapse rates through domain selection and spatial temperature correction

We evaluated two methods of accounting for spatial variability of lapse rates: a spatial clustering approach and a

spatial temperature correction. Spatial clustering aims to identify contrasting regional climates which may merit separate lapse rates whereas the spatial temperature correction is designed to address gradual climatic gradients not related to elevational differences. Therefore, we recommend assessing the potential for clustering first, and then spatial correction. Spatial correction can be applied with or without clustering.

The clustering analysis identified two clusters roughly corresponding to stations west and east of the Cascade crest, hereafter referred to as a windward 'west' cluster ($n = 17$) and a leeward 'east' cluster ($n = 13$) (Figure 8a). Tmax lapse rates from these clusters contrasted with lapse rates from the full population of stations (Figure 8b). 'East' cluster lapse rates were steeper than full population or 'west' cluster lapse rates, except in winter. The 'east' cluster had the greatest seasonality, with steeper lapse rates during summer and weaker lapse rates in winter when inversions are more common (Whiteman *et al.*, 2001). The large uncertainty in the 'east' cluster may be partly due to the small elevation range of these stations (645 m) relative to those in the 'west' cluster (1,615 m), since small elevation ranges amplify the effects of non-elevational factors on the lapse rate. In contrast, 'west' cluster lapse rates were around $-5°C\ km^{-1}$ with minimal seasonality. The east–west contrasts in lapse rates and in lapse rate seasonality are similar to the results of Minder *et al.*, (2010) for the Washington Cascades. Coherent spatial patterns of lapse rates and lapse rate seasonality have also been identified in other regions including Spain and Northern Italy (Rolland, 2003; Navarro-Serrano *et al.*, 2018).

In all seasons except winter, the median Tmax lapse rate from the full population was weaker than the median lapse rate from either of the clusters. This was most evident in summer, when 'east' stations were significantly warmer than 'west' stations at the same elevation due to greater Bowen ratio and downward surface shortwave flux. The fact that the full population lapse rates do not represent the lapse rates in these subregions (similar to Rolland, 2003), and the strong and physically reasonable contrasts between 'east' and 'west' lapse rates motivate regionalization efforts when calculating lapse rates over large geographic areas.

Spatial correction of Tmax (T_{sc}) steepened lapse rates in the 'east' cluster, particularly in summer and generally reduced the uncertainty compared to lapse rates based on raw station temperatures and increased the correlation between elevation and temperature (Figure 8b). An exception was the 'east' cluster in winter, likely because of the prevalence of persistent winter cold pool events in this region (Whiteman *et al.*, 2001) which decouple near-

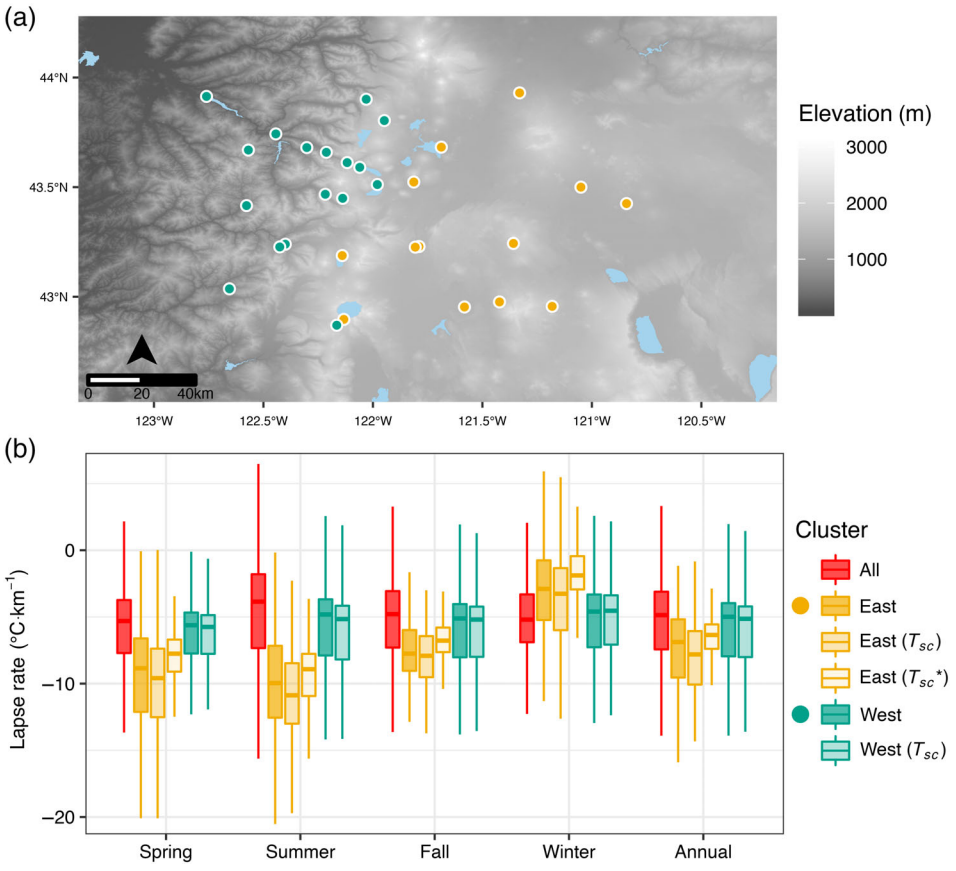

FIGURE 8 (a) Oregon Cascades domain with stations coloured according to cluster, as indicated by boxplot legend. (b) Tmax lapse rates estimated via SLR from samples of five stations from the full dataset ('all', $n = 30$), the 'west' cluster ($n = 17$), and the 'east' cluster ($n = 13$). Tsc indicates lapse rates estimated for the 'east' and 'west' clusters using spatially corrected station temperatures. Tsc* indicates lapse rates estimated from spatially corrected temperatures from the 'east' cluster with influential stations removed ($n = 12$)

surface temperatures from free-air temperatures. Considering all combinations of region, season, and sample size, T_{sc} reduced the lapse rate uncertainty in >75% of cases. The uncertainty reduction was typically on the order of tenths of °C km^{-1}, but in some cases exceeded 1°C km^{-1}. The uncertainty reduction was greater for small samples and in summer as free-air temperatures in summer exhibit a longitudinal gradient across the study region. Similarly, we expect that the uncertainty reduction would be greater if applied to regions with larger differences in free-air temperature (e.g., larger geographic regions).

While clustering was most appropriate for this example, we also assessed the benefit of applying the spatial correction without clustering. Lapse rates estimated from spatially corrected temperatures from samples of 5 stations from the full dataset were generally steeper and had lower uncertainty than those estimated from uncorrected station temperatures (not shown). The largest improvements were seen in summer; the median lapse rate was 0.9°C km^{-1} steeper and the IQR was 0.3°C km^{-1} smaller. These results were similar to the clustering results, but the improvements were smaller.

3.2.4 | Influential stations in the Oregon Cascades dataset

Application of Cook's Distance to the 'east' cluster identified the highest elevation station, Crater Lake COOP station (GHCND ID: USC00351946), as influential. This station was colder in every season than would be expected based on lapse rates estimated from the other stations and would be excluded by the TDA if the TDA did not try to maximize sample elevation range. It is possible that this station could be indicative of a steeper lapse rate across high elevation portions of the domain, however this would require additional data to evaluate. We excluded this station from further analysis, which resulted in lapse rates that were 1.5–3°C km^{-1} weaker than lapse rates based on the full cluster (Figure 8b). We reapplied Cook's Distance after removing this station and no additional influential stations were identified. Hereafter, the 'east' cluster refers to the 'east' cluster with this influential station removed.

3.2.5 | Application of topoclimatic dissimilarity approach to the Oregon Cascades dataset

Application of the TDA to the Oregon Cascades dataset, using spatially corrected station temperatures and sample sizes roughly 80% of the population size (13 and 10 for 'west' and 'east', respectively), resulted in contrasting lapse rate distributions across dissimilarity quantiles (Figure 9). The distributions of lapse rates in the most similar quantile were tightly clustered relative to distributions for less similar quantiles, suggesting that accounting for topoclimatic variability in station siting can improve temperature estimates (Lookingbill and Urban, 2003). In general, we expect the TDA to exclude dissimilar stations and reduce lapse rate error and uncertainty, however the specifics of which stations are excluded based on which covariates will depend on the dataset.

For the 'west' cluster in summer, cloud cover was the strongest predictor of temperature after elevation. In the most similar decile of samples, the TDA preferentially excluded the stations with the lowest and highest cloud cover values which were much warmer and cooler, respectively, than expected, resulting in a weaker lapse rate. The most important non-elevation predictor of winter temperature in the 'west' cluster was distance from coast, however this variable was strongly correlated with elevation ($r = 0.78$) limiting the TDA from excluding this covariate in station selection for the most similar decile. Instead, stations with extreme values in the next most important predictors of temperature (the waterbody index and the 40 km windex) were excluded from the most similar decile.

The 'east' cluster lapse rates based on the TDA had greater seasonality than the 'west' cluster. Summer lapse rates for the 'east' cluster were steep, with a median of −9.0°C km^{-1} for the most similar decile. This was slightly weaker than the summer lapse rate calculated across all 'east' cluster stations (−9.2°C km^{-1}) but is slightly steeper than the summer lapse rates found by Minder *et al.*, (2010) for the lee side of the Washington Cascades. In the most self-similar decile of samples, the TDA excluded a site that was an outlier in terms of the 40 km windex, which was the covariate most strongly correlated with summer temperature ($r = -0.56$) after elevation ($r = -0.80$). Winter temperatures were as strongly correlated with the TCI as they were with elevation ($r \sim 0.41$), corroborating the importance of inversions and cold-air drainage effects in the 'east' cluster in winter. The TDA preferentially excluded the station with the highest TCI value from the most similar decile of samples.

4 | DISCUSSION

Our results document latent uncertainties in near-surface temperature lapse rate estimates. Standard approaches for calculating lapse rates using our example of stations in the Oregon Cascades showed uncertainty

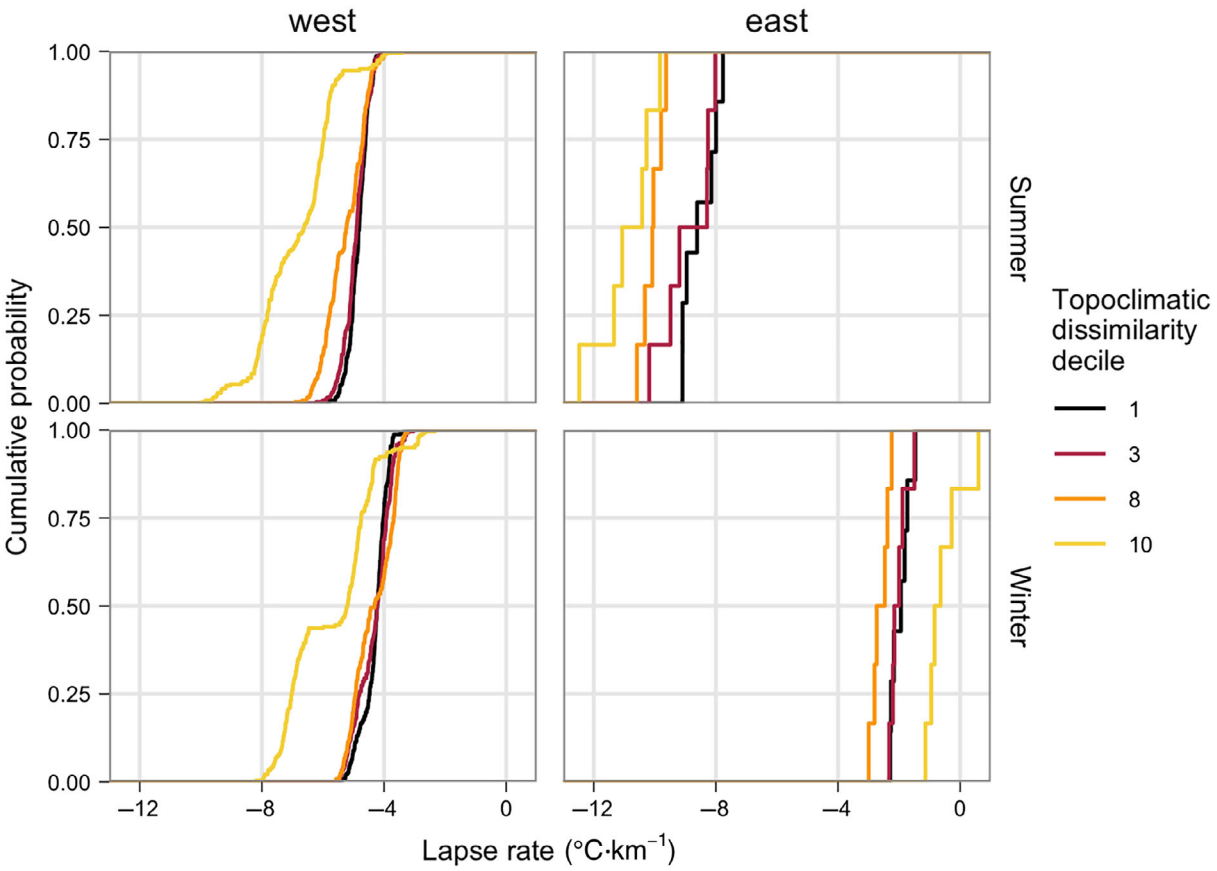

FIGURE 9 Cumulative distributions of spatially corrected Tmax lapse rates estimated from samples of stations from the 'west' (left column) and 'east' (right column) clusters of the Oregon Cascades dataset for summer and winter (rows). Sample sizes of 13 and 10 were used for the 'west' and 'east' clusters, respectively. Results are grouped by decile of the dissimilarity metric. Only deciles 1, 3, 8, and 10 are shown

of >5°C km^{-1} in some cases (Figure 7). Given this uncertainty, it is unsurprising that the mean environmental lapse rate of −6.5°C km^{-1} is often used. However, the sensitivity of environmental models to lapse rate estimates (e.g., Gardner and Sharp, 2009) indicates that a one size fits all lapse rate parameter is not sufficient and that better lapse rate estimation methods are needed (e.g., Minder *et al.*, 2010). The analyses presented above of observational and synthetic datasets point to a handful of best practices for lapse rate estimation (Figure 10) applicable to any timescale or geographic context, and to station data or gridded data (Cannon *et al.*, 2012).

1 *Estimation method*: SLR provides more accurate and robust lapse rate estimates than MLR in situations with high collinearity and data noise or small sample sizes (Figure 4). MLR can provide extreme lapse rate estimates when collinearity exists, which is common in observational data (Figures 7 and S1). Therefore, we recommend the use of SLR.
2 *Sample size*: Small samples are more sensitive than large samples to deviations in station temperature stemming from non-elevational factors. Evaluation of the TDA found that sample sizes that were roughly 80% of the population size struck a balance between the benefits of more data points and the benefits of being able to exclude dissimilar stations (Figure 6). We recommend using more than 5 stations and using sample sizes of about 80% of the population size when applying the TDA.
3 *Elevation Range*: Theory and exploratory data analysis indicate that lapse rate error increases dramatically as the sample elevation range decreases (Figure 8). Efforts should be made to collect data from a wide range of elevations, or barring this, a large number of stations, and the greater lapse rate uncertainty stemming from small elevation ranges should be taken into account in broader modelling efforts.
4 *Dataset Noise*: Analysis of the synthetic datasets illustrated that dataset noise increases lapse rate uncertainty and can increase bias (Figure 3). Efforts

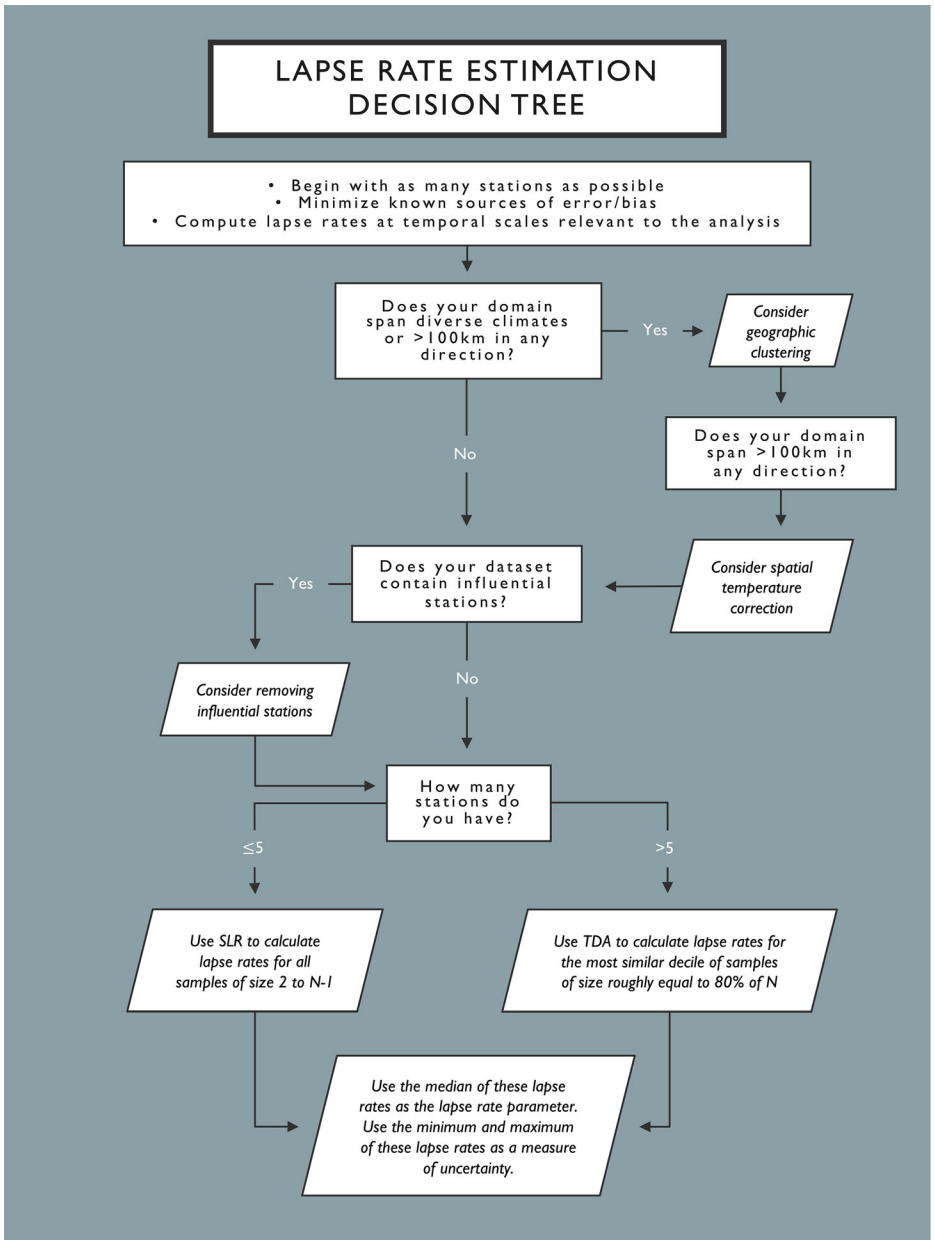

FIGURE 10 Decision tree outlining best practices for estimating near-surface temperature lapse rates. N is the total number of stations available (i.e., the population size)

to quality control and correct for known sources of temperature bias, including removing influential stations, can reduce the uncertainty in lapse rate estimates.

5 *Collinearity*: Collinearity of elevation with non-elevational factors influencing temperature is common in observational data and affects lapse rate estimates (Figures 3 and 4). Selection of self-similar samples (e.g., using the TDA) can reduce the effects of collinearity and improve lapse rate estimates (Figures 5 and 6). Topoclimatic variables used to assess collinearity and sample self-similarity should be tailored to reflect processes relevant to the region and time period of interest.

6 *Domain selection*: Lapse rates estimated from windward and leeward clusters of stations showed distinct values and seasonality compared to those using stations from the full domain (Figure 8). This suggests that lapse rates should be estimated over regions without strong climatic discontinuities or should be estimated from spatially corrected temperatures.

7 *Uncertainty*: Given the large uncertainty in lapse rates documented here, we argue that lapse rate uncertainty should be incorporated in model uncertainty and sensitivity analyses when possible.

Using the best practices outlined above we estimated seasonal lapse rates and lapse rate uncertainty for the

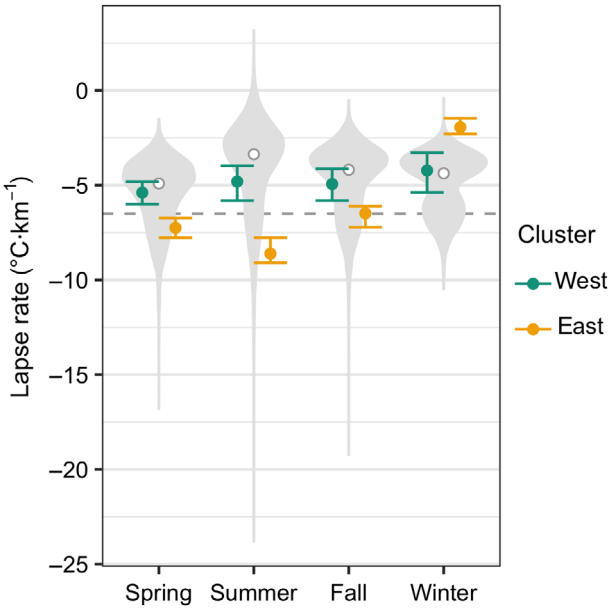

FIGURE 11 Seasonal Tmax lapse rates estimated for the Oregon Cascades stations following best practices. Coloured points represent the single best lapse rate (i.e., the median lapse rate of the most similar decile of samples) and coloured bars indicate uncertainty range (the minimum and maximum lapse rates of the most similar decile of samples). Grey violin plots illustrate the possible lapse rates that can be estimated from any combination of 10 stations from the original dataset, not using best practices. White dots indicate the lapse rate estimated from the full 30 station dataset not using best practices. The grey dashed line marks the MELR (−6.5 °C km^{-1})

'west' and 'east' clusters of the Oregon Cascades station data (Figure 11). Our results indicate lapse rates close to 2°C km^{-1} different, on average, from those estimated from the full dataset without using best practices or from the commonly used MELR (similar to Navarro-Serrano *et al*., 2018; Shen *et al*., 2016).

5 | CONCLUSIONS

Temperature fields in environmental models dictate a wide range of processes including phenology, growing degree days, precipitation phase, snowmelt, and glacier mass balance, thereby exerting outsized influence on modelling outcomes. Yet these temperature fields are often governed by a single lapse rate parameter selected from the literature or calculated from a handful of stations within the modelling domain with little consideration of error or uncertainty. Contrasting but physically reasonable lapse rates (−4 and -6.5°C km^{-1}) applied to an elevational range of 1 km can result in differences in model outcomes that are of similar magnitude to the difference between modelling outcomes based on historical and +2°C climate scenarios (Minder *et al*., 2010), emphasizing the importance of carefully choosing a lapse rate. We show that lapse rate uncertainty can easily exceed the range evaluated by Minder *et al*., (2010), suggesting that the effects of lapse rate uncertainty may exceed the effects of climate change in some modelling contexts.

The best practices presented here reduce lapse rate uncertainty and error, but further research is needed to refine lapse rate estimation methods. In particular, nighttime temperature lapse rates in complex terrain remain difficult to determine due to localized atmospheric decoupling, and thermal belts at topographic elevations near the inversion top may lead to multiple lapse rates (Lundquist and Cayan, 2007). Building on the clustering analysis presented here, additional work is needed to understand the relevant spatial scales over which lapse rates should be defined. Development of carefully designed observational temperature networks may help to further evaluate methodological choices. Improvement in lapse rate estimates will enhance the accuracy of environmental models and downscaling routines, enabling better understanding of biophysical processes and how they will change in a warming climate.

ACKNOWLEDGEMENTS

The authors have no conflicts of interest. ACL was supported by the National Science Foundation's IGERT Program (award 1249400). The authors thank three reviewers for their insightful comments which improved this manuscript.

ORCID

A. C. Lute https://orcid.org/0000-0002-0469-3831
John T. Abatzoglou https://orcid.org/0000-0001-7599-9750

REFERENCES

Abatzoglou, J.T., Redmond, K.T. and Edwards, L.M. (2009) Classification of regional climate variability in the state of California. *Journal of Applied Meteorology and Climatology*, 48(8), 1527–1541. https://doi.org/10.1175/2009JAMC2062.1.

Altman, N. and Krzywinski, M. (2016) Analyzing outliers: influential or nuisance? *Nature Methods*, 13(4), 281–282. https://doi.org/10.1038/nmeth.3812.

Blandford, T.R., Humes, K.S., Harshburger, B.J., Moore, B.C., Walden, V.P. and Ye, H. (2008) Seasonal and synoptic variations in near-surface air temperature lapse rates in a Mountainous Basin. *Journal of Applied Meteorology & Climatology*, 47(1), 249–261. https://doi.org/10.1175/2007JAMC1565.1.

Cannon, A.J., Neilsen, D. and Taylor, B. (2012) Lapse rate adjustments of gridded surface temperature normals in an area of

complex terrain: atmospheric reanalysis versus statistical upsampling. *Atmosphere-Ocean*, 50(1), 9–16. https://doi.org/10.1080/07055900.2011.649035.

Cook, R.D. (1977) Detection of influential observation in linear regression. *Technometrics*, 19(1), 5.

Daly, C., Gibson, W., Taylor, G., Johnson, G. and Pasteris, P. (2002) A knowledge-based approach to the statistical mapping of climate. *Climate Research*, 22, 99–113. https://doi.org/10.3354/cr022099.

Daly, C., Conklin, D.R. and Unsworth, M.H. (2010) Local atmospheric decoupling in complex topography alters climate change impacts. *International Journal of Climatology*, 30, 1857–1864. https://doi.org/10.1002/joc.2007.

Daly, C., Halbleib, M., Smith, J.I., Gibson, W.P., Doggett, M.K., Taylor, G.H., Curtis, J. and Pasteris, P.P. (2008) Physiographically sensitive mapping of climatological temperature and precipitation across the conterminous United States. *International Journal of Climatology*, 28(15), 2031–2064. https://doi.org/10.1002/joc.1688.

Dobrowski, S.Z., Abatzoglou, J.T., Greenberg, J. and Schladow, S.G. (2009) How much influence does landscape-scale physiography have on air temperature in a mountain environment? *Agricultural and Forest Meteorology*, 149, 1751–1758. https://doi.org/10.1016/j.agrformet.2009.06.006.

Dormann, C.F., Elith, J., Bacher, S., Buchmann, C., Carl, G., Carré, G., Marquéz, J.R.G., Gruber, B., Lafourcade, B., Leitão, P. J., Münkemüller, T., McClean, C., Osborne, P.E., Reineking, B., Schröder, B., Skidmore, A.K., Zurell, D. and Lautenbach, S. (2013) Collinearity: a review of methods to deal with it and a simulation study evaluating their performance. *Ecography*, 36(1), 27–46. https://doi.org/10.1111/j.1600-0587.2012.07348.x.

Gardner, A.S. and Sharp, M. (2009) Sensitivity of net mass-balance estimates to near-surface temperature lapse rates when employing the degree-day method to estimate glacier melt. *Annals of Glaciology*, 50(50), 80–86. https://doi.org/10.3189/172756409787769663.

Gardner, A.S., Sharp, M.J., Koerner, R.M., Labine, C., Boon, S., Marshall, S.J., Burgess, D.O. and Lewis, D. (2009) Near-surface temperature lapse rates over Arctic glaciers and their implications for temperature downscaling. *Journal of Climate*, 22(16), 4281–4298. https://doi.org/10.1175/2009JCLI2845.1.

Graham, M.H. (2003) Confronting multicollinearity in ecological mutliple regression. *Ecology*, 84(11), 2809–2815. https://doi.org/10.1890/02-3114.

Harding, R.J. (1979) Altitudinal gradients of temperature in the Northern Pennines. *Weather*, 34(5), 190–202. https://doi.org/10.1002/j.1477-8696.1979.tb03442.x.

Immerzeel, W.W., Petersen, L., Ragettli, S. and Pellicciotti, F. (2014) The importance of observed gradients of air temperature and precipitation for modeling runoff from a glacierized watershed in the Nepalese Himalayas. *Water Resources Research*, 50 (3), 2212–2226. https://doi.org/10.1002/2013WR014506.

Kattel, D., Yao, T., Yang, K., Tian, L., Yang, G. and Joswiak, D. (2013) Temperature lapse rate in complex mountain terrain on the southern slope of the Central Himalayas. *Theoretical & Applied Climatology*, 113(3/4), 671–682. https://doi.org/10.1007/s00704-012-0816-6.

Kirchner, M., Theresa, F.-K., Gert, J., Michael, L., Ludwig, R., Hans-Eckhart, S. and Peter, S. (2013) Altitudinal temperature lapse rates in an Alpine valley: trends and the influence of season and weather patterns. *International Journal of Climatology*, 33(3), 539–555. https://doi.org/10.1002/joc.3444.

Li, X., Wang, L., Chen, D., Yang, K., Xue, B. and Sun, L. (2013) Near-surface air temperature lapse rates in the mainland China during 1962–2011. *Journal of Geophysical Research: Atmospheres*, 118(14), 7505–7515. https://doi.org/10.1002/jgrd.50553.

Lookingbill, T.R. and Urban, D.L. (2003) Spatial estimation of air temperature differences for landscape-scale studies in montane environments. *Agricultural and Forest Meteorology*, 114(3–4), 141–151. https://doi.org/10.1016/S0168-1923(02)00196-X.

Lundquist, J.D. and Cayan, D.R. (2007) Surface temperature patterns in complex terrain: daily variations and long-term change in the Central Sierra Nevada, California. *Journal of Geophysical Research: Atmospheres*, 112(D11), D11124. https://doi.org/10.1029/2006JD007561.

Lundquist, J.D., Pepin, N. and Rochford, C. (2008) Automated algorithm for mapping regions of cold-air pooling in complex terrain. *Journal of Geophysical Research: Atmospheres*, 113(D22), D22107. https://doi.org/10.1029/2008JD009879.

Mason, C.H. and Perreault, W.D., Jr. (1991) Collinearity, power, and interpretation of multiple regression analysis. *Journal of Marketing Research*, 28(3), 268–280.

McCutchan, M.H. (1983) Comparing temperature and humidity on a mountain slope and in the free air nearby. *Monthly Weather Review*, 111, 836–845. https://doi.org/10.1175/1520-0493(1983)111<0836:CTAHOA>2.0.CO;2.

Menne, M.J., Durre, I., Vose, R.S., Gleason, B.E. and Houston, T.G. (2012) An overview of the global historical climatology network-daily database. *Journal of Atmospheric and Oceanic Technology*, 29(7), 897–910. https://doi.org/10.1175/JTECH-D-11-00103.1.

Minder, J.R., Mote, P.W. and Lundquist, J.D. (2010) Surface temperature lapse rates over complex terrain: lessons from the Cascade Mountains. *Journal of Geophysical Research: Atmospheres*, 115(D14), D14122. https://doi.org/10.1029/2009JD013493.

Montgomery, D.C., Peck, E.A. and Vining, G.G. (2012) *Introduction to linear regression analysis*. Hoboken, NJ: John Wiley & Sons, Inc.

Navarro-Serrano, F., López-Moreno, J.I., Azorin-Molina, C., Alonso-González, E., Tomás-Burguera, M., Sanmiguel-Vallelado, A., Revuelto, J. and Vicente-Serrano, S.M. (2018) Estimation of near-surface air temperature lapse rates over continental Spain and its mountain areas. *International Journal of Climatology*, 38(8), 3233–3249. https://doi.org/10.1002/joc.5497.

Pepin, N., Benham, D. and Taylor, K. (1999) Modeling lapse rates in the maritime uplands of northern England: implications for climate change. *Arctic, Antarctic, and Alpine Research*, 31(2), 151–164. https://doi.org/10.2307/1552603.

Pepin, N., Bradley, R.S., Diaz, H.F., Baraer, M., Caceres, E.B., Forsythe, N., Fowler, H., Greenwood, G., Hashmi, M.Z., Liu, X. D., Miller, J.R., Ning, L., Ohmura, A., Palazzi, E., Rangwala, I., Schöner, W., Severskiy, I., Shahgedanova, M., Wang, M.B., et al. (2015) Elevation-dependent warming in mountain regions of the world. *Nature Climate Change*, 5(5), 424–430. https://doi.org/10.1038/nclimate2563.

Rolland, C. (2003) Spatial and seasonal variations of air temperature lapse rates in alpine regions. *Journal of Climate*, 16(7),

1032–1046. https://doi.org/10.1175/1520-0442(2003)016<1032:SASVOA>2.0.CO;2.

Sadoti, G., McAfee, S.A., Roland, C.A., Fleur Nicklen, E. and Sousanes, P.J. (2018) Modelling high-latitude summer temperature patterns using physiographic variables. *International Journal of Climatology*, 38(10), 4033–4042. https://doi.org/10.1002/joc.5538.

Sekercioglu, C.H., Schneider, S.H., Fay, J.P. and Loarie, S.R. (2008) Climate change, Elevational range shifts, and bird extinctions. *Conservation Biology*, 22(1), 140–150. https://doi.org/10.1111/j.1523-1739.2007.00852.x.

Shen, Y.-J., Shen, Y., Goetz, J. and Brenning, A. (2016) Spatial-temporal variation of near-surface temperature lapse rates over the Tianshan Mountains, Central Asia. *Journal of Geophysical Research: Atmospheres*, 121(23), 14,006–14,017. https://doi.org/10.1002/2016JD025711.

Whiteman, C.D., Zhong, S., Shaw, W.J., Hubbe, J.M., Bian, X. and Mittelstadt, J. (2001) Cold pools in the Columbia Basin. *Weather and Forecasting*, 16, 16.

Wolfe, J. A. (1992). *An analysis of present-day terrestrial lapse rates in the western conterminous United States and their significance to paleoaltitudinal estimates* (Report No. 1964; Bulletin). USGS Publications Warehouse. https://doi.org/10.3133/b1964

SUPPORTING INFORMATION

Additional supporting information may be found online in the Supporting Information section at the end of this article.

How to cite this article: Lute AC, Abatzoglou JT. Best practices for estimating near-surface air temperature lapse rates. *Int J Climatol*. 2021;41 (Suppl. 1):E110–E125. https://doi.org/10.1002/joc.6668